Nuclear Engineering and Technology 57 (2025) 103865

Contents lists available at ScienceDirect

Nuclear Engineering and Technology

journal homepage: www.elsevier.com/locate/net

Original Article

Improved HUST-PTF beamline control system for beam commissioning

Chengyong Liu, Yu Chen, Dong Li *, Qushan Chen, Shaokun Zhou, Lingfeng Shu, Zhenyi Yang, Bin Qin

State Key Laboratory of Advanced Electromagnetic Technology, School of Electrical and Electronic Engineering, Huazhong University of Science and Technology, Wuhan, 430074, China

ARTICLE INFO

Keywords:
Proton therapy
OPC UA
Beamline control system
Database
Beam commissioning

ABSTRACT

Huazhong University of Science and Technology is constructing a proton therapy facility (HUST-PTF) utilizing a 240 MeV superconducting cyclotron. To control the beamline-related devices during beam transportation, a beamline control system (BCS) with a distributed architecture based on open platform communications unified architecture (OPC UA) was proposed. In the last version of BCS, there are some issues, such as thread blocking, low data refresh rate, and functional deficit. To overcome the mentioned drawbacks, this study optimizes the interaction between magnet power supplies and the BCS through thread flow optimization and a selective Monitor mechanism, introduces a denormalized beam database, and integrates the beam diagnostics subsystem into BCS. Finally, the improved BCS is validated on-site with a proton beam under different energy settings, demonstrating successful adherence to the design requirements.

1. Introduction

The proton therapy, characterized by the Bragg peak [1], is a crucial cancer treatment method that minimizes damage to normal tissues. The Huazhong University of Science and Technology is constructing a proton therapy facility (HUST-PTF) comprising a 240 MeV superconducting cyclotron, a beam transport line, and three treatment rooms (two rotating and one fixed) [2], as illustrated in Fig. 1 [3].

The detailed parameters of the facility are listed in Table 1. The proton beam is extracted from the cyclotron and transported to the treatment rooms via the beamline. This beamline incorporates hardware components, such as dipole magnets, quadrupole magnets, passive elements (a degrader, an energy slit, and collimators), beam diagnostics-related devices, etc. To facilitate communication and control of these components, a distributed control system, named the beamline control system (BCS), is designed and developed through the auto-configuration of distributed clients and data nodes.

Currently, there are various architectures to construct beamline control systems. For instance, the Experimental Physics and Industrial Control System (EPICS) [4] architecture is employed at facilities including the Center for Proton Therapy at the Paul Scherrer Institute (PSI) [5], the China Spallation Neutron Source (CSNS) [6], and Compact Laser Plasma Accelerator (CLAPA) at Peking University [7]. Similarly, the open platform communications unified architecture (OPC UA) [8] is utilized at MedAustron, the center for ion beam therapy and research [9].

Among the mentioned architectures, the OPC UA [10] is chosen for constructing the BCS. Although the OPC UA protocol's real-time performance is inferior to that of the Channel Access (CA) protocol used in EPICS, its enhanced scalability and improved security are key considerations. The OPC UA protocol enables the integration of new functionalities and services without requiring updates to the existing control system operations. It also incorporates robust security mechanisms, including authentication, encryption, and integrity protection.

In the first phase, the HUST-PTF BCS system framework [3] has been completed, but during the beam commissioning, some problems were found by users concerning the efficiency and stability of the existing system:

Regarding system stability, the existing system exhibited low fault tolerance, as subsystem disconnections resulted in main system failures. Specifically, during practical testing, the OPC UA server of the underlying power supply server's main thread interacts with multiple client sub-threads of power supplies for data exchange, which leads to communication disruptions caused by power outages or faults in certain power supplies, resulting in the corresponding TCP/IP client threads being blocked, which ultimately causes the collapse of the OPC UA server.

Concerning efficiency, low data refresh rates were observed,

* Corresponding author.
E-mail address: lidonghust@hust.edu.cn (D. Li).

https://doi.org/10.1016/j.net.2025.103865
Received 21 February 2025; Received in revised form 26 July 2025; Accepted 18 August 2025
Available online 19 August 2025

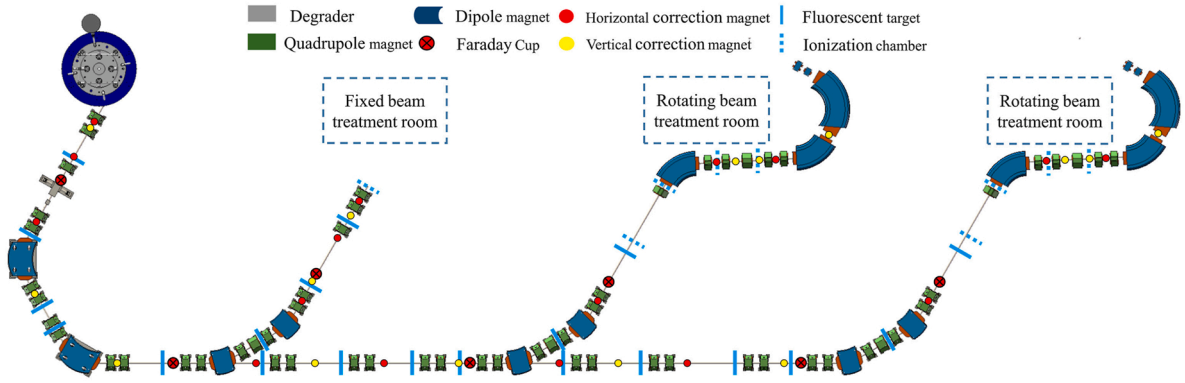

Fig. 1. The structure of HUST-PTF.

Table 1
The parameters of HUST-PTF.

Parameter	Value
Proton energy extracted from a cyclotron	240 MeV
Energy adjustment range of the degrader	70–230 MeV
Therapeutic beam current	0.4–4 nA
Single-step energy adjustment time	≤150 ms
Gantry rotation angle range	±180°
Isocenter positioning accuracy	≤0.5 mm
Maximum dose rate	3 Gy/L/min
Scanning method	Spot scanning
Scanning range	30 cm × 30 cm

attributed primarily to the system's architecture, which encompasses numerous magnet power supplies and employs a combined OPC UA Monitor and Read mechanism, causing contention between the read and monitor queues. To be specific, when the power supply current changes, a cyclic Read mechanism is employed to improve the refresh rate, which has been proven effective in testing with virtual power supplies [3]. However, when applied to actual magnet power supplies, the response times for read or write commands were notably slower compared to the virtual ones. This discrepancy led to delays in accessing the Monitor's data queue and hindered the timely processing of the newly introduced cyclic read data queue.

Additionally, the current BCS is hindered by the lack of an efficient database for storing and retrieving relevant calculated and detected data, which obstructs the rapid parameter configuration essential for the treatment process. Furthermore, it struggles to effectively control the beam diagnostics subsystem, which consists of interdependent distributed device servers, thereby rendering control via a single client impractical due to the complexity.

To overcome the mentioned problems, we improve the existing BCS

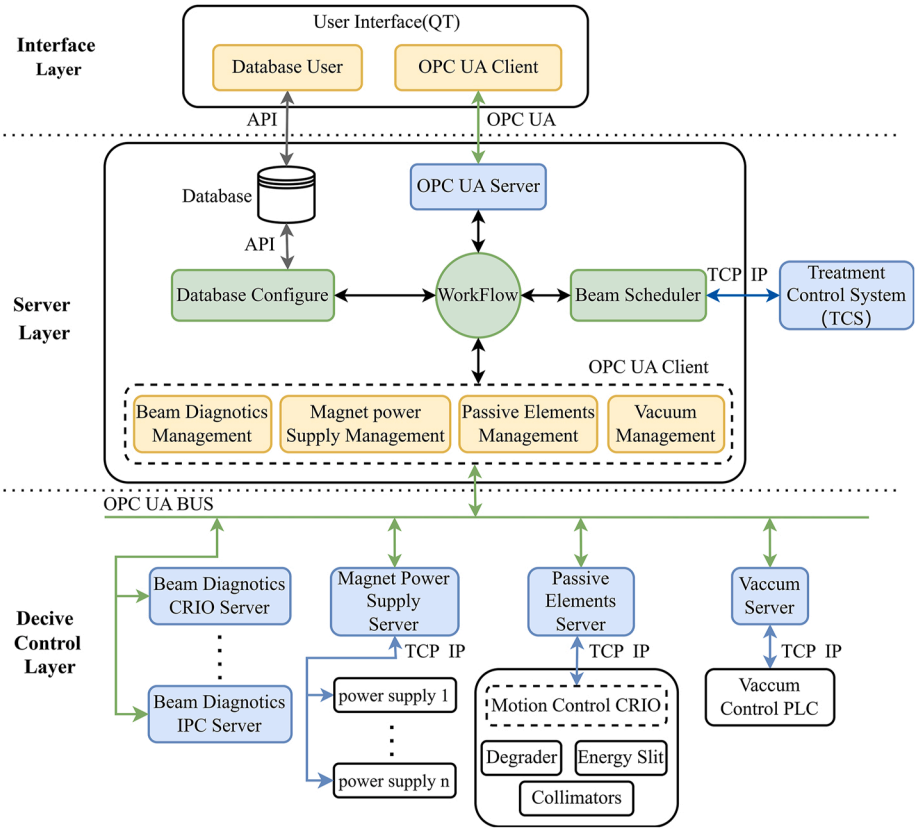

Fig. 2. Overview of Improved BCS architecture.

using the following strategies:

1. We adopt a multi-threaded magnet power supply control method, where each thread interacts with its corresponding power supply independently, managed by the OPC UA server. Moreover, we optimized the event flow of each thread's interaction with the magnet power supplies, adding a specially designed mechanism for power supply disconnection detection and reconnection.
2. We use a selective Monitor mechanism to interact with the magnet power supplies, which directly monitors parts of the power supplies or parts of their data, thereby reducing the data queue and improving the refresh rate of the power supply data.
3. We integrate a denormalized database into the existing BCS based on My Structured Query Language (MySQL) [11], which stores related data together. This approach reduces table join operations and cross-node data transfer, thereby significantly accelerating queries and enhancing the BCS's database operation performance. Besides, the improved BCS system can effectively control beam diagnostics devices through the auto-configuration of distributed clients and data nodes.

It is important to note that, unlike previous studies relying exclusively on physical simulations for the HUST-PTF beamline [2], this study presents the experimental results obtained during beam commissioning using the BCS, while also validating part of the simulated results in Ref. [12].

The remainder of this study is organized as follows: Section II provides an overview of BCS; Section III outlines related modifications and details. Section IV examines the experimental results. Section V discusses prospects and current limitations. Finally, Section VI provides the conclusion.

2. Overview of the BCS architecture

The BCS adopts a distributed control architecture, including three layers: device control, server, and interface, as shown in Fig. 2.

Their specific functions are as follows:

1. The device control layer consists of OPC UA servers dedicated to magnet power supplies, beam diagnostics devices, a vacuum subsystem, and passive elements. This layer facilitates interaction with the physical beamline devices and publishes data as OPC UA variables to its corresponding OPC UA server.
2. The server layer is governed by the Workflow, which manages Database Configure, Beam Scheduler, Management of devices, and other subsystems across three modes: Standby, Beam Commissioning, and Therapy. In Therapy mode, the workflow allows all subsystem functions but restricts the interface's operational access. The operation of each subsystem is fully managed by the workflow. During the treatment process, the BCS interacts with the Treatment Control System (TCS) via the Beam Scheduler. Based on the treatment requirements of the TCS, such as energies and gantry angles, the workflow automatically schedules the subsystems to query the database and configure device parameters.
3. The interface layer, constructed using the open-source Qt framework, provides graphical user Interfaces for detecting and operating various beamline subsystems and interacts with the server layer via the OPC UA client and the database.

This study provides only a concise overview of the optimization strategy within the overall architectural framework. For a comprehensive discussion of the detailed functionalities and system architecture, readers are referred to Ref. [3].

Table 2
The parameters of magnet power supplies.

Category	Model (referring to output voltage and current)	Ripple of output current	Stability of the current	Adjustment resolution	Linearity
Dipole Quadrupole Corrector	480A/130V 300A/35V 150A/20V 20A/20V	≤±10 ppm	≤±25 ppm (20 %–100 %)	≥18 bit	≤±10 ppm

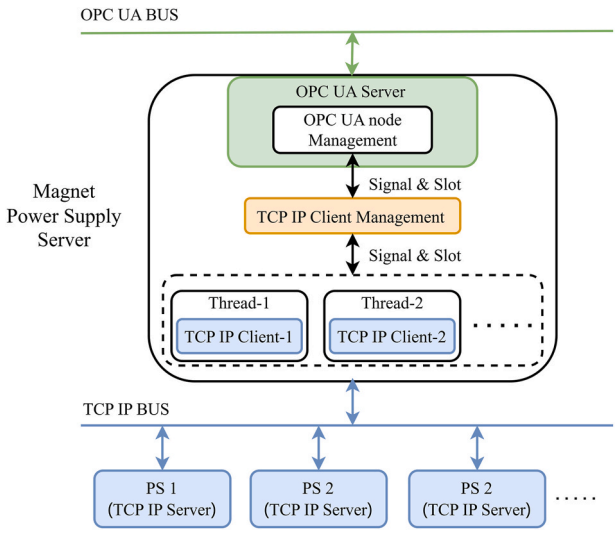

Fig. 3. Architecture of the magnet power supply server.

3. Optimization and integration of the BCS for beam commissioning

3.1. Magnet power supply

A total of 104 magnet power supplies are used in the HUST-PTF, all of which are direct current (DC) power supplies. These are mainly divided into three categories: dipole magnet power supplies, quadrupole magnet power supplies, and corrector magnet power supplies. The relevant specifications are shown in Table 2.

Each power supply is configured as a TCP/IP server, with the underlying server established. As shown in Fig. 3, the OPC UA node management is in charge of managing the data transmission across the entire server. As each magnet power supply requires a TCP/IP client to facilitate interaction, OPC UA node Management cannot manage all clients and read data simultaneously. Therefore, each TCP/IP client is placed in a separate thread, with a TCP/IP Client Management to oversee them. When OPC UA Management receives data read and write tasks from the upper layer, TCP/IP Client Management dispatches these tasks to the corresponding TCP/IP Client in its thread, allowing each client to perform operations independently. This approach delegates numerous tasks from OPC UA node management to various threads, thereby reducing the load and enhancing the efficiency of data read and write [13].

However, during subsequent real power supply tests, power outages in some power supplies disrupted communication, causing the collapse of the magnet power supply server. As shown in Fig. 4 (a), any loss of power supply communication results in the corresponding thread's inability to clear the task queue. This failure prevents client management from completing tasks, which in turn causes node management to become blocked. Given the single-threaded nature of the OPC UA server,

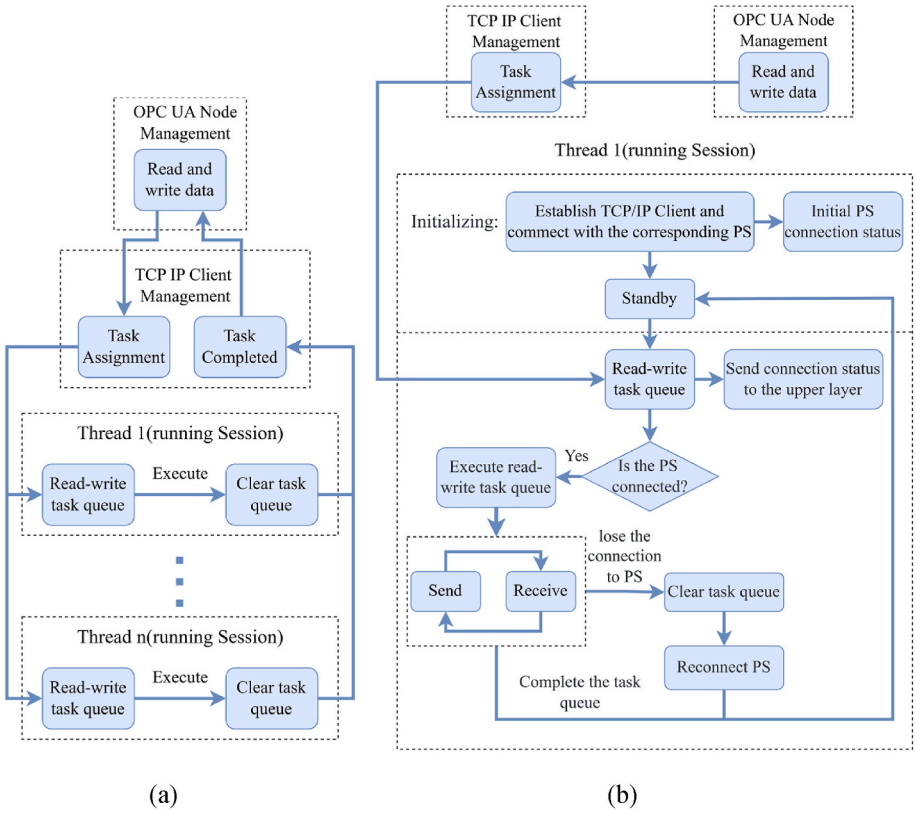

Fig. 4. (a). The overall task execution flow. (b). The task execution flow of a power supply thread.

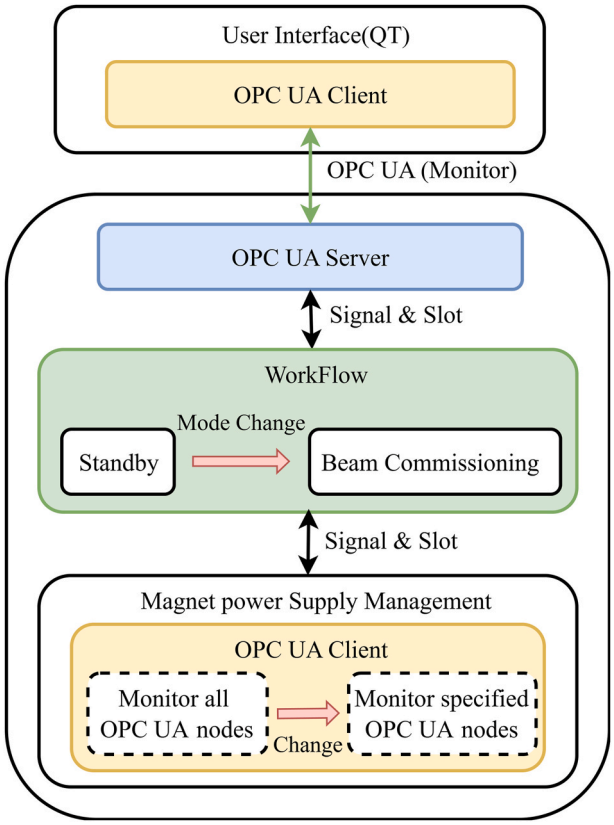

Fig. 5. The operational mechanism of selective monitoring.

this internal node management block ultimately leads to the server's collapse. To improve the fault tolerance performance of the system, the task execution flow of each thread's TCP/IP Client is optimized, and mechanisms for disconnection detection and reconnection are added. The optimized task execution process, shown in Fig. 4 (b), assigns each thread a Session (a C++ class) to manage tasks. During initialization, each TCP/IP client connects to the power supply and retrieves its connection status. Tasks from OPC UA node management are added to a queue, which is cleared if communication is lost, triggering a reconnection attempt. If the connection is stable, tasks are executed in a "send-receive" cycle monitored by a timer. Multiple timeouts clear the queue to avoid thread blockage. This optimization prevents server freezes and ensures disconnection events are promptly reported to the upper layer and displayed on the interface.

Furthermore, low data refresh rates were observed. However, the previously designed Monitor and Read mechanism to improve the refresh rate was not effective in testing with actual power supplies. Therefore, a selective Monitor mechanism is implemented to access power supply data effectively. Each magnet power supply contains 23 data points associated with 23 OPC UA nodes, covering a total of 104 power supplies. However, not all data from these power supplies is necessary. The selective Monitoring mechanism can adjust the monitoring queue to detect only the relevant data from specific power supplies. For instance, only the status and real-time output current of the power supply are required during the beam commissioning.

As shown in Fig. 5, when the BCS transfers to beam commissioning mode, only the OPC UA nodes corresponding to the power supply's status and real-time current are monitored. This approach directly reduces the data interaction queue, thereby increasing the data refresh rate.

3.2. *Database in BCS*

As depicted in Fig. 2, the BCS architecture incorporates a server-layer

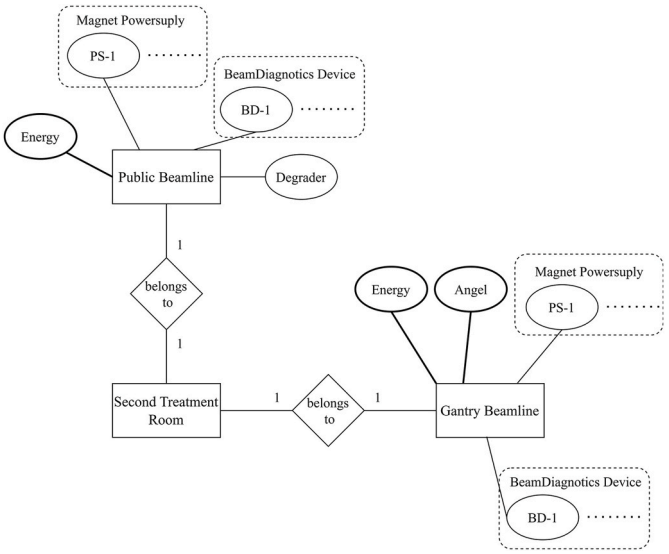

Fig. 6. ER model of the Second Treatment Room.

database primarily responsible for storing beamline device data during the HUST-PTF beam commissioning. This stored data forms the basis for subsequent beam commissioning and treatment phases. Rapid access to magnet currents and degrader positions across various energy settings and gantry angles within the treatment rooms is essential for these processes. To expedite data retrieval, treatment rooms and energy settings are abstracted as entities within an Entity-Relationship (ER) model, illustrated in Fig. 6, with magnet power supplies, beam diagnostic devices, and degrader as attributes.

Unlike conventional normalized databases, the applied denormalized approach minimizes the number of tables, thereby enhancing data retrieval speed by reducing the need for table joins. Despite potential issues with data redundancy and writing in denormalized databases, this ER model effectively separates common beamline and gantry segments, thereby avoiding redundancy in beamline data related to gantry angles. Furthermore, since data writing occurs only during beam commissioning, the demands on writing performance are minimal.

Based on the defined ER model, the open-source MySQL database system is selected for its efficient management and high-concurrency handling capabilities. This model stores single-datatype attributes, such as magnet currents and degrader positions, and multi-faceted data for beam diagnostic components, including beam size and position. Therefore, the JavaScript Object Notation (JSON) [14] is adopted for data storage, which structures data as key-value pairs, allowing all information from a beam diagnostic device to be encapsulated within a single object. When retrieval is required, the corresponding data can be obtained by extracting and decoding the complete JSON object. The resulting schema is structured into five principal tables, with the fixed treatment room containing a single table, while each of the two rotating treatment rooms is equipped with two tables: a public beamline and a gantry beamline.

Following database establishment, both read and write operations are required. Given that the BCS is implemented in C++, MySQL Connector/C++ 8.0 is selected to facilitate the connection between the BCS and the database. MySQL Connector C++ 8.0 provides a user-based approach for database access via its Application Programming Interface (API). At the interface layer, a read-only user is created, and a cross-platform API is employed to access the database at the server layer. Conversely, at the server layer, the database configuration utilizes the root user, possessing full permissions for local database access. As a result, when modifications to the database are required, instructions are sent from the interface layer to the server layer, and changes can only be executed following Workflow checks, significantly enhancing database security. Additionally, relevant database operations and sub-interfaces are incorporated at the interface layer to facilitate database reading and writing for related engineers.

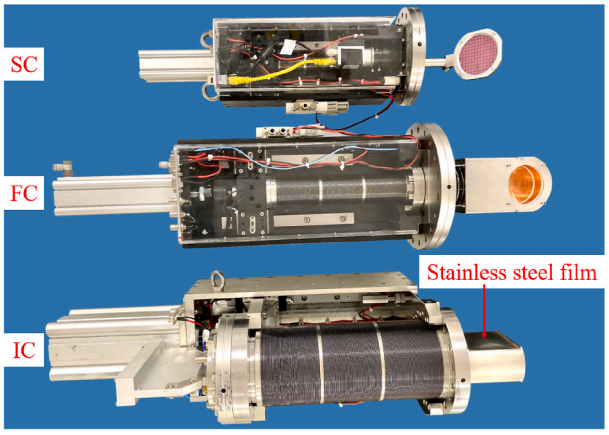

Fig. 7. Prototypes of the SC, FC and thick IC in HUST-PTF [15].

Table 3
The parameters of three beam diagnostic devices.

Detector	Specification
Scintillation screen	CCD camera resolution: 2 MP Lens fixed focal length: 16 mm Diameter of the circular target: 62 mm Distance between the lens and the screen: 200 mm Actual resolution: 0.08 mm/pixel
Faraday cup	Material: oxygen-free copper Data refresh rate of the slow mode: 4 Hz Data refresh rate of the flash mode: 5 kHz Maximum nonlinear error: 1.1 %
Ion chamber	Cathode frame area: 60 × 60 mm^2 Cathode frame pitch: 1 mm Cathode frame strip width: 0.8 mm Bias high voltage: ≤2 kV Maximum refresh rate: 2 kHz

3.3. Beam diagnostics

The beam diagnostic devices of HUST-PTF are primarily divided into three types: the Scintillation screen (SC), Faraday cup (FC), and Ion chamber (IC) [15], which detect the beam image, intensity, and profile information, respectively, as shown in Fig. 7. All three types of detectors are interceptive detectors, and their relevant specifications are presented in Table 3.

These three types of beam diagnostic devices have been installed on the beamline of HUST-PTF and are controlled by an industrial control computer and CRIOs, which publish data to the OPC UA server for external interaction. Therefore, BCS does not need to set up an OPC UA server for protocol conversion. However, the distribution of device control for beam diagnostics is relatively complex. As depicted in Fig. 8, a single industrial control computer manages all SCs and pneumatic devices controlling the insertion and removal of all beam diagnostic devices, while each CRIO controls either two FCs or one IC.

Therefore, the design and implementation of dedicated beam diagnostic management modules are necessary.

As illustrated in Fig. 9, corresponding OPC UA clients are implemented for each distinct beam diagnostic OPC UA server, with each client operating within a separate thread. And, the configuration of distributed clients and data nodes is managed by the OPC UA Client Schedule. When Beam Diagnostics Management receives a data read/write command, the OPC UA Client Schedule queries the OPC UA

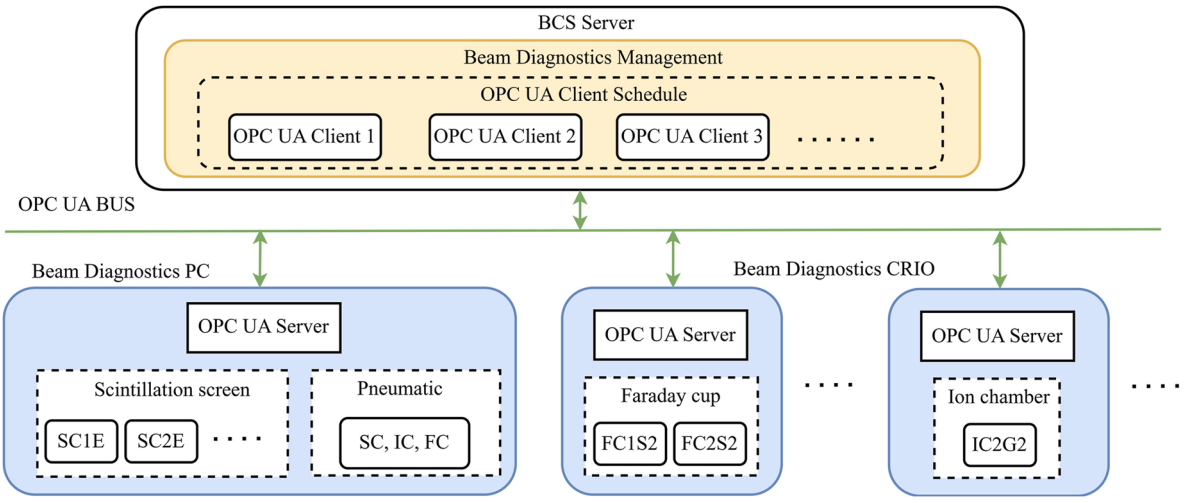

Fig. 8. Architecture of beam diagnostics server.

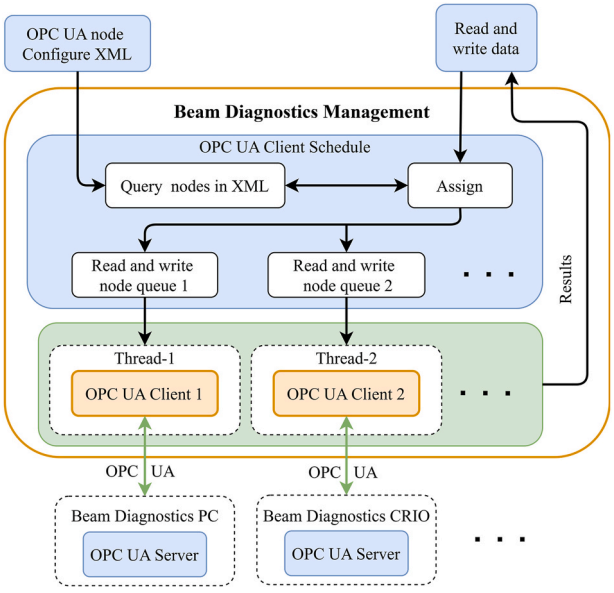

Fig. 9. Architecture of beam diagnostics management.

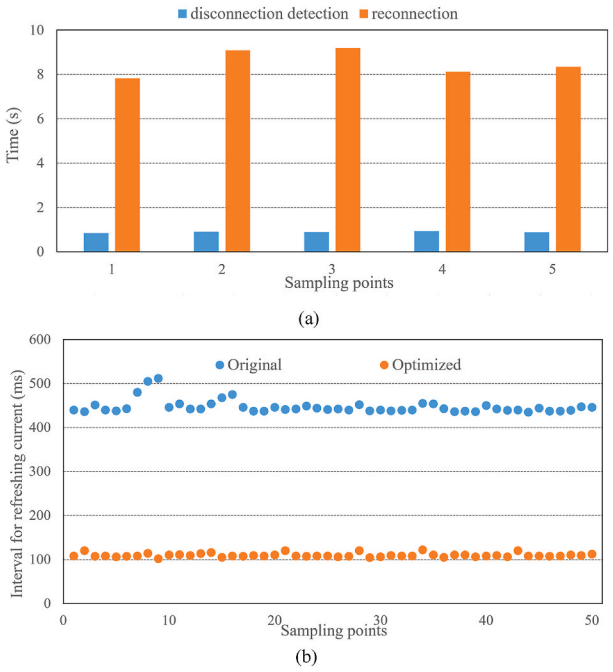

Fig. 10. Test Result of the Magnet Power Supply. (a). fault tolerance test. (b). refresh interval test.

configuration node ID in XML format and sends the data read/write queue to different clients. Then, each OPC UA client executes the read or write operations based on the assigned tasks and transmits the results back. Finally, upper-level modules and beam diagnostic sub-interfaces are developed based on actual interaction data acquired from the beam diagnostic system.

4. Experimental results of BCS during beam commissioning

4.1. Magnet power supply

To evaluate the system's fault tolerance, during actual power supply tests, the IP address of a specific power supply is altered and then restored using configuration software to simulate network disconnection and reconnection, with the time taken being recorded. This duration is compared to the time detected by the BCS for power disconnection and reconnection. As depicted in Fig. 10 (a), the server continues to operate normally, detecting the disconnection within 1 s, transmitting the information to the interface, and successfully re-establishing the connection within 8 s after power supply restoration.

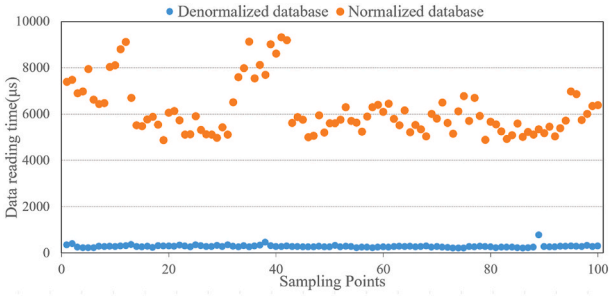

Fig. 11. Result of database reading performance.

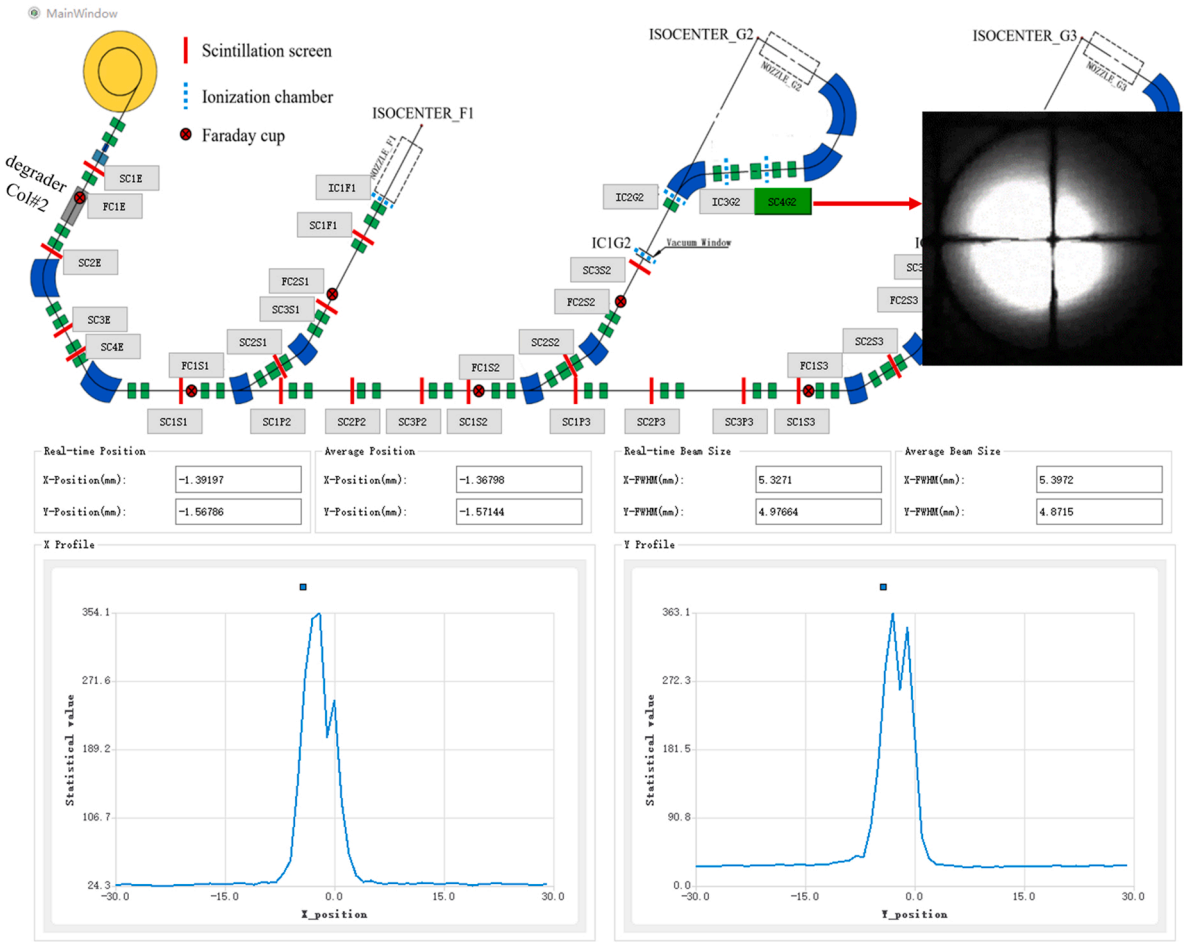

Fig. 12. Beam diagnostics interface of BCS.

Furthermore, as shown in Fig. 10 (b), by directly reading the current data from the power supply, the selective monitoring mechanism reduces the data refresh interval from the original 450 ms–100 ms.

4.2. Beam database

To evaluate the performance of the denormalized beam database, a normalized database is created, with one table per device: 104 power supply tables, 30 beam diagnostic tables, and one degrader table. Both databases store all device parameters for energy settings ranging from 70 to 240 MeV (in 1 MeV increments) and angles from −180° to +180° (in 1° increments). Performance comparison is conducted by retrieving device parameters for the first rotating treatment room. In the denormalized database, querying only two tables and identifying the relevant device columns is sufficient to retrieve device parameters for various energy and angle settings. In contrast, the normalized database requires querying 41 power supply tables and one degrader table to retrieve the same information. As illustrated in Fig. 11, this optimization reduces data reading time from approximately 6 ms in the normalized database to 300 μs in the denormalized database.

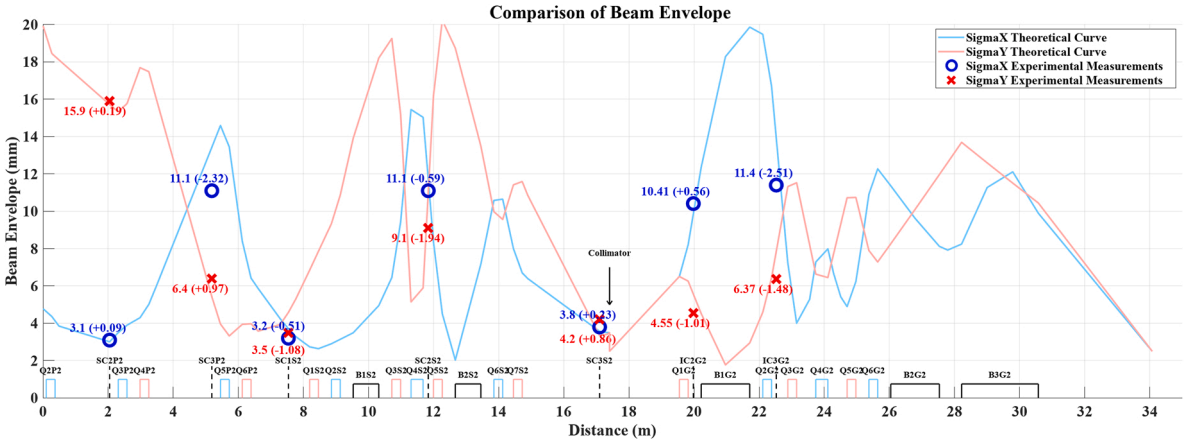

Fig. 13. Comparison of actual beam parameters and the designed values.

4.3. Beam diagnostics and optical result

To verify that the Beam Diagnostics subsystem can meet the requirements of beam commissioning, an experimental test is conducted in HUST-PTF, which injected a 239.8 MeV, 1 nA (actual measurement) proton beam from the accelerator to the beamline.

As shown in Fig. 12, by referencing theoretical calculations and actual beam measurement results to correct the current values of the magnet power supply, the proton beam is successfully transported to the final scintillation screen, SC4G2. And, the proton beam's central position and size are optimal, enabling delivery to the first rotating treatment room.

Subsequently, passive elements are employed to control beam energy from 239.8 MeV to 210 MeV and beam quality (i.e., emittance and dispersion). The measured beam spot size obtained from beam diagnostic devices is compared with theoretical simulations [12] computed using the TRANSPORT code [16] from Q2P2 to IC3G2.

During initial beam commissioning, while dipole magnet power supplies are operated at their theoretical current settings, significant beam loss occurs in the vacuum chamber. This phenomenon is attributed to discrepancies between the actual and theoretical B-I characteristics of the dipole magnets. Therefore, current adjustments are implemented to optimize beam transmission efficiency while ensuring that the beam is at the center of the track through the dipole magnets. Through iterative optimization of dipole magnet currents, experimental data demonstrate excellent agreement with theoretical models. As illustrated in Fig. 13, the maximum observed discrepancy between measured and theoretical values of Sigma X and Sigma Y across all diagnostic devices remained within 3 mm, indicating strong consistency between experimental results and theoretical expectations.

5. Conclusion and discussion

This study, considering the original drawbacks of HUST-PTF, optimizes the magnet power supplies, beam diagnostics, passive elements, and beamline vacuum sections within the BCS and develops a denormalized database for the storage and retrieval of device information for beam commissioning. The improved BCS is verified, and the results indicate that it can effectively manage beamline control tasks.

After the optimizations, the BCS can meet the requirements of actual beam commissioning, but there are still many areas for improvement. Specifically, to enhance system stability, the development of a dedicated safety interlock system for hardware protection is required. Additionally, to optimize treatment efficiency, the implementation of synchronous triggering is proposed to reduce power configuration time, complementing the time-saving benefits of the denormalized database architecture described in this study. Current analyses reveal persistent discrepancies between design specifications and actual beam parameters. Future work will explore the integration of automated beam commissioning within the BCS framework and the application of digital twin technology to refine the commissioning process and address these observed deviations.

CRediT authorship contribution statement

Chengyong Liu: Writing – original draft, Visualization, Software, Methodology, Investigation, Formal analysis, Data curation, Conceptualization. **Yu Chen:** Writing – original draft, Formal analysis, Data curation. **Dong Li:** Writing – review & editing, Writing – original draft, Validation, Supervision, Methodology, Investigation, Conceptualization. **Qushan Chen:** Validation, Supervision. **Shaokun Zhou:** Software, Investigation. **Lingfeng Shu:** Software, Methodology. **Zhenyi Yang:** Writing – review & editing. **Bin Qin:** Writing – review & editing, Validation, Supervision, Project administration, Funding acquisition.

Declaration of competing interest

The authors declare that they have no known competing financial interests or personal relationships that could have appeared to influence the work reported in this paper.

Acknowledgments

This work was supported by the National Key Research and Development Program of China (No. 2016YFC0105305) and the National Natural Science Foundation of China (11975107).

References

[1] M. Cianchetti, M. Amichetti, Sinonasal malignancies and charged particle radiation treatment: a systematic literature review, Int. J. Otolaryngol. 2012 (1) (2012) 325891.
[2] B. Qin, X. Liu, Q.-S. Chen, D. Li, W.-J. Han, P. Tan, Z.-Q. Zhang, C. Zhou, A.-T. Chen, Y.-C. Liao, et al., Design and development of the beamline for a proton therapy system, Nucl. Sci. Tech. 32 (12) (2021) 138.
[3] P. Li, D. Li, B. Qin, C. Zhou, W. Han, Y. Liao, A. Chen, Design of hust-ptf beamline control system for fast energy changing, Nucl. Eng. Technol. 54 (8) (2022) 2852–2858.
[4] Epics. https://epics.anl.gov/index.php.
[5] D. Anicic, M. Gasche, H. Lutz, T. Korhonen, A. Mezger, Upgrading the proscan control system to epics: a success story, in: Proceedings of ICALEPCS, 2009.
[6] Y. Zhang, D. Jin, P. Zhu, Y. He, X. Wu, M. Kang, F. Guo, L. Wang, G. Li, W. Gao, et al., The accelerator control system of csns, Rad. Detection Technol.Methods 4 (2020) 478–491.
[7] Y. Xia, Q. Wang, J. Zhao, L. Feng, E. Guo, T. Yang, Y. Wang, F. Li, Z. Guo, Q. He, K. Chen, Y. Lu, X. Yan, C. Lin, Design and implementation of epics on the laser accelerator: clapa-I control system upgrade, IEEE Trans. Nucl. Sci. 71 (1) (2024) 18–30.
[8] OPC UA. https://opcfoundation.org/about/opc-technologies/opc-ua/.
[9] J. Gutleber, R. Moser, The medaustron accelerator control system: design installation and commissioning, in: 14th International Conference on Accelerator and Large Experimental Physics Control Systems, March 6–11, 2013, p. TUCOAAB04. San Francisco, CA, USA, https://cds.cern.ch/record/1697002, 2013.
[10] OPC UA SDK. https://www.unified-automation.com/.
[11] MySql. https://www.mysql.com/cn/.
[12] Y. Chen, B. Qin, X. Liu, W. Wang, Y. Liao, Start-to-end modeling and transmission efficiency optimization for a cyclotron-based proton therapy beamline, Nucl. Eng. Technol. 56 (10) (2024) 4365–4374.
[13] C. Zhou, D. Li, W. Han, B. Qin, Development of a power supply control system and virtual simulation based on docker, in: 2020 IEEE 1st China International Youth Conference on Electrical Engineering (CIYCEE), 2020, pp. 1–7.
[14] Json. https://www.json.org/json-zh.html.
[15] A. Chen, Q. Chen, X. Liu, C. Zhou, D. Li, B. Qin, X. Kang, Z. Xu, M. Li, K. Tang, R. Mao, Prototype development of the beam diagnostic system of a proton therapy facility based on a superconducting cyclotron, Nucl. Instrum. Methods Phys. Res. Sect. A Accel. Spectrom. Detect. Assoc. Equip. 998 (2021) 165208.
[16] U. Rohrer, "PSI Graphic Transport Framework".